JACC: CARDIOVASCULAR IMAGING VOL. 1, NO. 3, 2008

ISSN 1936-878X/08/$34.00
PUBLISHED BY ELSEVIER INC. DOI:10.1016/j.jcmg.2008.01.013

Cardiovascular Magnetic Resonance Characterization of Mitral Valve Prolapse

Yuchi Han, MD,* Dana C. Peters, PHD,* Carol J. Salton, BA,* Dorota Bzymek, RDCS,* Reza Nezafat, PHD,* Beth Goddu, RT(R)(MR),* Kraig V. Kissinger, RT(R)(MR),* Peter J. Zimetbaum, MD,* Warren J. Manning, MD,*† Susan B. Yeon, MD, JD*

Boston, Massachusetts

OBJECTIVES This study sought to develop cardiovascular magnetic resonance (CMR) diagnostic criteria for mitral valve prolapse (MVP) using echocardiography as the gold standard and to characterize MVP using cine CMR and late gadolinium enhancement (LGE)-CMR.

BACKGROUND Mitral valve prolapse is a common valvular heart disease with significant complications. Cardiovascular magnetic resonance is a valuable imaging tool for assessing ventricular function, quantifying regurgitant lesions, and identifying fibrosis, but its potential role in evaluating MVP has not been defined.

METHODS To develop CMR diagnostic criteria for MVP, characterize mitral valve morphology, we analyzed transthoracic echocardiography and cine CMR images from 25 MVP patients and 25 control subjects. Leaflet thickness, length, mitral annular diameters, and prolapsed distance were measured. Two- and three-dimensional LGE-CMR images were obtained in 16 MVP and 10 control patients to identify myocardial regions of fibrosis in MVP.

RESULTS We found that a 2-mm threshold for leaflet excursion into the left atrium in the left ventricular outflow tract long-axis view yielded 100% sensitivity and 100% specificity for CMR using transthoracic echocardiography as the clinical gold standard. Compared with control subjects, CMR identified MVP patients as having thicker (3.2 $\pm$ 0.1 mm vs. 2.3 $\pm$ 0.1 mm) and longer (10.5 $\pm$ 0.5 mm/m^2 vs. 7.1 $\pm$ 0.3 mm/m^2) indexed posterior leaflets and larger indexed mitral annular diameters (27.8 $\pm$ 0.7 mm/m^2 vs. 21.5 $\pm$ 0.5 mm/m^2 for long axis and 22.9 $\pm$0.7 mm/m^2 vs. 17.8 $\pm$ 0.6 mm/m^2 for short axis). In addition, we identified focal regions of LGE in the papillary muscles suggestive of fibrosis in 10 (63%) of 16 MVP patients and in 0 of 10 control subjects. Papillary muscle LGE was associated with the presence of complex ventricular arrhythmias in MVP patients.

CONCLUSIONS Cardiovascular magnetic resonance image can identify MVP by the same echocardiographic criteria and can identify myocardial fibrosis involving the papillary muscle in MVP patients. Hyperenhancement of papillary muscles on LGE is often present in a subgroup of patients with complex ventricular arrhythmias. (J Am Coll Cardiol Img 2008;1:294–303) © 2008 by the American College of Cardiology Foundation

From the *Department of Medicine (Cardiovascular Division) and the †Department of Radiology, Beth Israel Deaconess Medical Center, Harvard Medical School, Boston, Massachusetts. Dr. Manning received a research grant that was >$10,000 from Philips Medical Systems. The work is supported in part by the Warren-Whitman-Richardson Fellowship (Harvard Medical School) awarded to Dr. Han.

Manuscript received November 2, 2007; revised manuscript received January 4, 2008, accepted January 15, 2008.

Mitral valve prolapse (MVP) is a common disorder afflicting 2% to 3% of the general population and is the most common cause of severe nonischemic mitral regurgitation (MR) requiring surgery in the U.S. (1). Mitral valve prolapse is defined by echocardiography as a condition in which segment(s) of 1 or both mitral leaflets extend above the plane of the mitral annulus in the parasternal long-axis view during ventricular systole by at least 2 mm (2,3).

See page 304

Mitral valve prolapse has been extensively studied by echocardiography, including two-dimensional (2D) and three-dimensional (3D) transthoracic echocardiography (TTE) and transesophageal echocardiography (2–7). Transthoracic echocardiography remains the diagnostic modality of choice for MVP because of its ease of use and unsurpassed temporal resolution. However, TTE imaging is highly dependent on patient image windows and the MR assessment is limited by its semiquantitative nature. Three-dimensional TTE provides excellent visualization of the prolapsed leaflets, but the limitations of echocardiography remain. Cardiovascular magnetic resonance (CMR) is a noninvasive imaging method with unlimited imaging planes that provides reproducible quantitative data on cardiac anatomy and function (8,9). Cine CMR methods allow for characterization of the valve morphology, and velocity encoded CMR provides for quantification of MR (10–12). In addition, CMR also provides a method to assess myocardial fibrosis. A recent study (13) compared cine CMR assessment of mitral valve morphology to transesophageal echocardiography and surgical findings, but the criteria for MVP in CMR was not developed.

Major complications such as progressive MR requiring valvular surgery and ventricular arrhythmia and sudden death are predominantly associated with the subgroup of patients with myxomatous valves (14,15), which are characterized by diffuse leaflet thickening, elongation, redundancy, and in some cases ruptured chordae tendineae (16). These characteristics of the mitral valve leaflets would be important to assess in MVP patients. In the patients who ultimately go to surgery, pre-operative characterization of prolapsed scallops (according to the Carpentier classification [17]) has significant implications for the complexity of surgical repair because the repair rates are lower in anterior leaflet prolapse (18–20). Transesophageal echocardiography is usually used for reliable scallop assessment; however, due to its moderately invasive nature, it is not universally performed prior to surgery. Because CMR is capable of imaging in multiple planes, it may reliably visualize individual scallops noninvasively.

The increased risk of atrial and ventricular tachyarrhythmias in myxomatous MVP patients can be as high as 50% to 60%, and there is a risk (0.4% to 2% per year) of sudden death in these patients (15,21,22). The relevance of these arrhythmias to the risk of sudden death remains uncertain. A number of young sudden death victims with MVP are asymptomatic females without significant MR (23,24). Perivalvular ventricular fibrosis and papillary muscle fibrosis have been well described in pathological studies (23,25). Additional reports have described scarring of the papillary muscles attributed to abnormal tension and subsequent ischemia of papillary muscles (26). Perivalvular and papillary muscle fibrosis in MVP patients has not been assessed in vivo and its relationship to ventricular tachyarrhythmias has not been examined.

We sought to develop CMR diagnostic criteria for MVP, characterize mitral valve morphology, and use 3D high-resolution late gadolinium enhancement (LGE)-CMR imaging (27) to visualize regions of myocardium with characteristics suggestive of fibrosis in MVP patients.

ABBREVIATIONS AND ACRONYMS

2C = two chambers
2D = two-dimensional
3D = three-dimensional
4C = four chambers
CMR = cardiovascular magnetic resonance
CVA = complex ventricular arrhythmia
ECG = electrocardiogram
EF = ejection fraction
LGE = late gadolinium enhancement
LV = left ventricular
LVOT = left ventricular outflow tract
MAD = mitral annular diameter
MR = mitral regurgitation
MVP = mitral valve prolapse
SSFP = steady state free processing
TTE = transthoracic echocardiography

METHODS

Patient selection. A query of our clinical TTE and CMR database identified 24 patients from 2004 to 2006 with CMR and TTE studies within 12 months of each other. Data from 12 patients were excluded due to prior mitral valve surgery (2), other coexisting valvular disease (3) or heart disease (3), or poor TTE (3) or CMR (1) images. A total of 19 patients with MVP were prospectively enrolled in an institutional review board–approved protocol (5 patients) or referred by their cardiologists to undergo CMR under clinical indications (14 patients). Of the 19 patients, 6 were excluded from valve morphology analysis due to lack of TTE (3) or poor CMR (2) images or were included in the retrospective arm (1). All prospectively imaged MVP patients had no history of coronary artery disease, hypertension, diabetes, or other intrinsic cardiomyopathies. We selected a control group of 25 patients with absence of valvular disease (mild grade MR was allowed). Of the 19

prospective patients, 3 with no (1) or poor (2) high-resolution 3D LGE-CMR were excluded in LGE analysis. Of the 25 control patients, 2 had high-resolution 3D LGE-CMR performed. An additional 8 normal control patients who had 3D LGE-CMR were included in LGE analysis.

Echocardiography. Transthoracic 2D and Doppler echocardiographic examinations were performed with a 3.5-MHz probe on a Vivid 7 ultrasonographic unit (GE Vingmed Ultrasound AS, Horten, Norway). Parasternal long-axis, apical 4-chamber (4C), and 2-chamber (2C) views were obtained as part of the routine clinical assessment.

CMR. The CMR imaging was performed using an Achieva 1.5-T MR whole body scanner (Philips Medical Systems, Best, the Netherlands) equipped with a 5-element cardiac synergy coil. Breath-hold retrospectively electrocardiogram (ECG)-gated cine steady state free processing (SSFP) images were acquired in the 2C and 4C horizontal long-axis views, and a short axis stack covering the entire left ventricle (8-mm slices with 2-mm gaps) as previously described (8,9). The left ventricular outflow tract (LVOT) long-axis view (Fig. 1), equivalent to the TTE parasternal long-axis view, was obtained by prescribing an image plane perpendicular to the mitral annular major axis centered at the aortic outflow track. In prospectively imaged MVP patients, a stack of cine SSFP images with 7-mm slice thickness with no gap in the LVOT view were obtained to cover the entire mitral valve (Fig. 2A). Sequence parameters were repetition time 3 ms, echo time 1.5 ms, flip angle 60°, field-of-view 320 mm, matrix 160 × 160. Temporal resolution was 30 to 35 ms. Free-breathing, ECG-triggered phase contrast velocity sequences for aortic flow oriented in the axial plane at the level of the bifurcation of the pulmonary artery were acquired as previously described (12).

Fifteen minutes after 0.2 mmol/kg intravenous administration of gadolinium-diethylenetriamine penta-acetic acid (Magnevist, Berlex/Schering AG, Berlin, Germany), ECG-gated breath-hold 2D LGE-CMR was performed in the 2C, 4C, and short axis orientations corresponding to the SSFP cine slices as previously described (28). Scan parameters were repetition time 4.3 ms, echo time 2.1 ms, flip angle 15°, field-of-view 320 mm, matrix 160 × 160, spatial resolution 2 × 2 × 8 mm^3 reconstructed to 1.2 × 1.2 × 8 mm^3 using zero-padding. At 20 min after injection, an ECG-gated free breathing, respiratory navigator-gated 3D LGE-CMR scan was obtained as previously described (27). Scan parameters were repetition time 5.6 ms, echo time 2.7 ms, flip angle 25°, field-of-view 320 mm, full echo, matrix 224 × 224 × 23 to 32 partition-encoded lines, spatial resolution 1.3 × 1.3 × 5 mm^3 reconstructed to 0.6 × 0.6 × 2.5 mm^3. For both 2D and 3D LGE-CMR scans, fat saturation was applied and inversion times were determined using the Look-Locker sequence (29).

Image analysis. The TTE image analysis was performed by a blinded experienced observer (DB) on EchoPACS Dimension (BT06, GE Vingmed Ul-

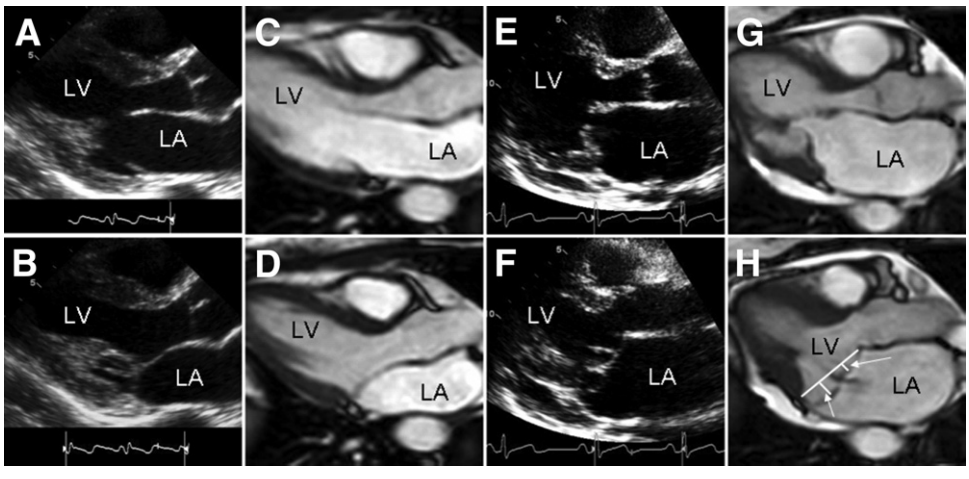

Figure 1. Comparison of the Long-Axis View in Control and MVP Patients by TTE and CMR

Control **(A to D)** and mitral valve prolapse (MVP) **(E to H)** patients. The two-dimensional transthoracic echocardiography (TTE) parasternal long-axis views **(A, B, E, F)** and cardiovascular magnetic resonance (CMR) left ventricle (LV) outflow tract views **(C, D, G, H)**. **(A, C, E, G)** Diastole; **(B, D, F, H)** systole. In **panel H**, **arrows** indicate the prolapsed distance measured by the maximum distance of the prolapsed leaflet to the mitral annular plane. LA = left atrium.

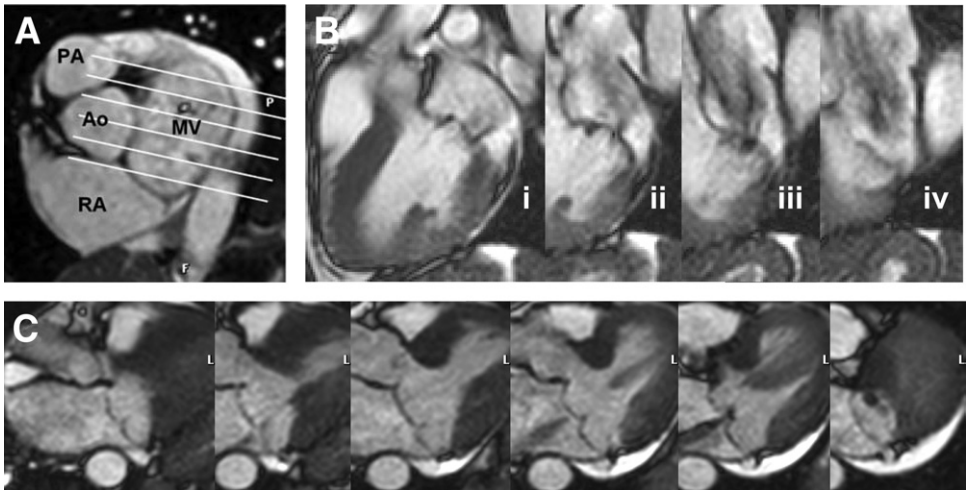

Figure 2. The LVOT Stack Prescription and 2 Examples

(A) Left ventricular outflow tract (LVOT) stack prescription is created by obtaining parallel slices across the mitral valve perpendicular to the long axis of the valve. **(B)** The LVOT stack from a patient with A1, P1, A2, and P2 prolapses. **(i)** A1/P1, **(ii)** and **(iii)** A2/P2, **(iv)** A3/P3. **(C)** The LVOT stack from a patient with prolapse of all scallops and a centrally directed mitral regurgitation jet. Ao = aorta; MV = mitral valve; PA = pulmonary artery; RA = right atrium.

trasound AS, Horten, Norway). The CMR data were analyzed independently by a different blinded observer (C.J.S.) using VIEWFORUM (Release 4) software (Philips Medical Systems). For both TTE and CMR, the prolapsed distance was measured for each leaflet as the maximum excursion of the leaflet beyond the mitral annular plane as defined by a line connecting the inferolateral mitral annulus to the aortomitral junction during systole (Fig. 1H). Additional measurements performed included the diastolic maximum mitral leaflet thickness (Fig. 3A), length (Fig. 4A), and end-systolic mitral annular diameter (MAD). The greater of the 2C and 4C MAD was used to approximate the major MAD (Fig. 5A). The TTE end-systolic parasternal long-axis MAD or the CMR LVOT MAD were used to approximate the minor MAD (Fig. 5B). Mitral leaflet length and MAD were indexed to body surface area. The blood-to-leaflet contrast ratio was measured by obtaining the ratio of maximum and minimum signal intensity across the valve leaflet during diastole. The ejection fraction (EF) was calculated by tracing the end-diastolic and end-systolic left ventricular (LV) slice contours and

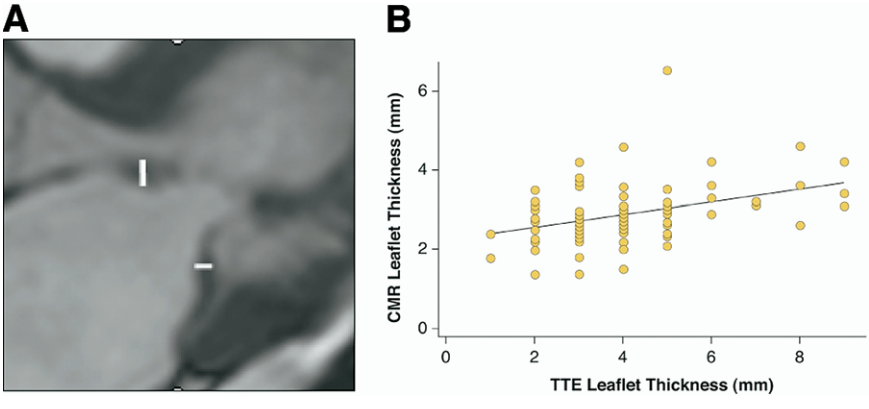

Figure 3. Mitral Leaflet Thickness

(A) The LVOT view showing leaflet thickness measurements obtained at the thickest portion of the leaflet during diastole. **(B)** Plot of all leaflets (including both anterior and posterior) by CMR versus TTE. **(Line)** Linear regression as described in text. The TTE measurements are generally higher than the CMR measurements. Abbreviations as in Figures 1 and 2.

JACC: CARDIOVASCULAR IMAGING, VOL. 1, NO. 3, 2008
MAY 2008:294–303

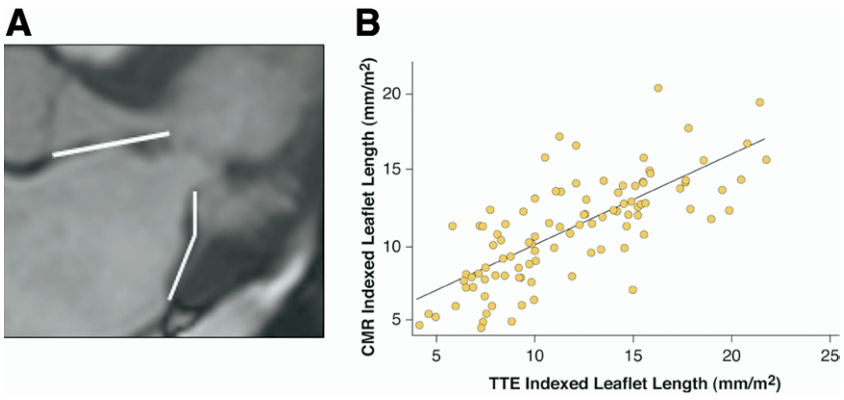

Figure 4. Indexed Mitral Leaflet Lengths

(A) The LVOT view showing both leaflet length measurements in diastole. **(B)** Plot of CMR versus TTE indexed leaflet length (including both anterior and posterior). **(Line)** Linear regression as described in text. Abbreviations as in Figures 1 and 2.

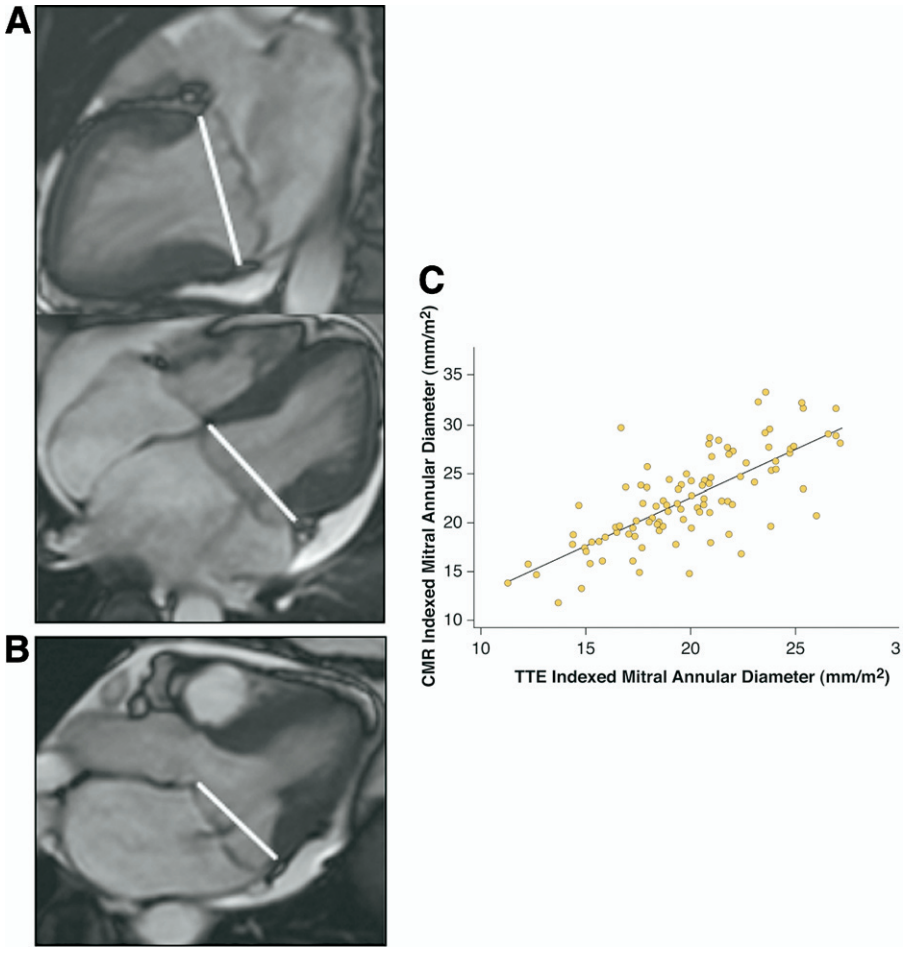

Figure 5. Indexed MADs

(A) The 2- and 4-chamber views of the end-systolic long-axis mitral annular diameter (MAD) measurement. **(B)** The LVOT view of the end-systolic short axis MAD measurement. **(C)** Plot of CMR versus TTE indexed MAD (including both long- and short-axis). **(Line)** Linear regression as described in text. Abbreviations as in Figures 1 and 2.

Table 1. Patient Characteristics for Mitral Valve Morphology

	Control (n = 25)	MVP (n = 25)	p Value
Age (yrs)	42.8 ± 11.0	50.9 ± 12.0	0.02
Male (%)	12 (48)	15 (60)	0.40
BSA (m^2)	1.87 ± 0.29	1.85 ± 0.20	0.80
EF (%)	60.8 ± 5.5	65.6 ± 6.7	0.01
MR			
0	18	0	
1+	7	2	
2+	0	4	
3+	0	14	
4+	0	5	

Values are mean ± standard deviation.
BSA = body surface area; EF = ejection fraction; MR = mitral regurgitation; MVP = mitral valve prolapse.

using the modified Simpson's rule method. The MR fraction was calculated as the difference between LV stroke volume and the forward aortic flow volume divided by the LV stroke volume (12).

The presence of abnormal LGE of the mitral valve was determined by the presence of extensive partial to complete ring-shaped high signal intensity (defined as 6 standard deviations higher than remote myocardium) in the short axis valve plane. Myocardial LGE was considered positive when part of the myocardial tissue present on the SSFP images was replaced by high signal intensity in the LGE images.

Arrhythmia analysis. Complex ventricular arrhythmia (CVA) was defined as Grade III or higher by the Lown and Wolf classification (30). Absence of CVA was determined by a negative Holter or event monitor, or by the absence of complaints of palpitations or skipped beats and no ambulatory ECG record of ventricular arrhythmias while being regularly followed by local cardiologists for at least 5 years.

Statistical analysis. Data are presented as mean ± standard deviation (for age, body surface area, and EF) or mean ± standard error of the mean (for measurements presented in Table 4). The sensitivity and the specificity of CMR identification of prolapse were determined using TTE as the gold standard. Data were analyzed using the 2-tailed Student's *t* test to compare continuous variables such as EF, body surface area, and age; the Wilcoxon rank sum test was used to compare categorical variables such as MR grade and gender. Fisher's exact test was used to test the relationship between LGE and CVA. Linear regression analyses were performed between CMR and TTE measurements. A p value of <0.05 was considered significant. All statistical analyses were performed with STATA version 10 (StataCorp, College Station, Texas).

RESULTS

Mitral valve morphology. The clinical characteristics of the MVP and control populations for mitral valve morphology analyses are summarized in Table 1. Gender and body surface area distributions were similar. The MVP cohort on average was slightly older and had a higher EF. Figure 1 demonstrates TTE and CMR images of a control subject and a MVP subject in the long-axis view during diastole and systole. The sensitivity and specificity for leaflet identification and MVP patient identification using 1-, 2-, and 3-mm leaflet displacements beyond the mitral annulus as cutoffs are summarized in Table 2. Using the criterion of at least 2-mm displacement, CMR had 100% sensitivity and specificity in identifying MVP patients (all 25 MVP patients correctly identified). On a per leaflet basis, the 2-mm criterion had 100% sensitivity and specificity for the posterior leaflet; the sensitivity was 78% and specificity was 97% for the anterior leaflet.

Identification of prolapsed scallops. By choosing a stack of cine SSFP images (Fig. 2A) perpendicular to the mitral valve major axis in the LVOT view, we can identify prolapsed scallops. Figure 2B shows an image from a patient with prolapse of 4 scallops on CMR (A1, A2, P1, and P2, but not A3 and P3), and Figure 2C shows an image from a patient with prolapse of all scallops and centrally directed MR jet. Cine images of this mitral valve can be seen in the Online Video.

Comparison of leaflet thicknesses. Measurements of leaflet thickness of MVP and control subjects by TTE and CMR are presented in Table 3. The CMR measurements of the posterior leaflet were

Table 2. Sensitivity and Specificity of CMR Diagnostic Criterion of MVP Using Cutoffs of 1 mm, 2 mm, or 3 mm of Leaflet Excursion Into the Left Atrium Beyond the Mitral Annulus

	1 mm (%)	2 mm (%)	3 mm (%)
Anterior leaflet			
Sensitivity	83	78	67
Specificity	90	97	97
Posterior leaflet			
Sensitivity	100	100	96
Specificity	100	100	100
Any leaflet			
Sensitivity	100	100	96
Specificity	96	100	100

CMR = cardiovascular magnetic resonance; other abbreviations as in Table 1.

significantly greater in the MVP patients as compared to the control subjects. We did not find the anterior leaflet thickness measurements to be significantly different by CMR in MVP patients as compared to controls, but the significant difference was found by TTE. Linear regression gave a best fit as CMR leaflet thickness = 2.3 mm + 0.16 × TTE leaflet thickness, with $R^2 = 0.153$, as shown in Figure 3B. There was significantly higher blood-to-leaflet contrast ratio of the leaflets from MVP patients compared to control patients by CMR ($p < 0.002$) (Table 3).

Comparison of leaflet lengths. The MVP patients had longer indexed posterior leaflets by both CMR and TTE, but we did not find the indexed anterior leaflet length to be significantly different from that of the control patients (Table 3). Linear regression gave a best fit as CMR indexed leaflet length = 4.1 mm/m^2 + 0.59 × TTE indexed leaflet length, with $R^2 = 0.548$, as shown in Figure 4B.

Table 3. Mitral Valve Characteristics of MVP and Control Patients by TTE and CMR

	TTE		CMR	
	Control (n = 25)	MVP (n = 25)	Control (n = 25)	MVP (n = 25)
Thickness				
(A) (mm)	3.5 ± 0.2	5.0 ± 0.3*	3.0 ± 0.1	3.2 ± 0.2†
(P) (mm)	2.6 ± 0.2	4.7 ± 0.4*	2.3 ± 0.1	3.2 ± 0.1*
Indexed length				
(A) (mm/m^2)	14.3 ± 0.6	15.6 ± 0.6†	13.0 ± 0.4	14.1 ± 0.5†
(P) (mm/m^2)	7.8 ± 0.4	9.6 ± 0.5*	7.1 ± 0.3	10.5 ± 0.5*
Indexed annulus				
(L) (mm/m^2)	18.3 ± 0.4	22.2 ± 0.5*	21.5 ± 0.5	27.8 ± 0.7*
(S) (mm/m^2)	17.1 ± 0.6	21.7 ± 0.6*	17.8 ± 0.6	22.9 ±0.7*
Blood-to-leaflet contrast ratio				
(A)	NA	NA	1.5 ± 0.1	2.2 ± 0.1*
(P)	NA	NA	1.3 ± 0.1	2.4 ± 0.2*

Values are mean ± standard error of mean. *$p < 0.01$ versus control. †p = nonsignificant versus control.
A = anterior; L = major axis; NA = not applicable; P = posterior; S = minor axis; TTE = transthoracic echocardiography; other abbreviations as in Tables 1 and 2.

Comparison of MADs. Both TTE and CMR found that MVP patients have greater MADs, as shown in Table 3. The CMR measurements were greater than TTE measurements for indexed major MAD in both control patients and MVP patients ($p < 0.0001$). Linear regression gave a best fit as CMR indexed MAD = 2.7 mm/m^2 + 0.99 × TTE indexed MAD, with $R^2 = 0.547$, as shown in Figure 5B.

LGE in the mitral valve. The presence of LGE on the valve and the mitral annulus was common in MVP patients with 15 of 16 (94%) partial or complete ring-shaped extensive LGEs on high-resolution 3D LGE-CMR imaging in the short axis view at the valve plane (Fig. 6). Extensive LGE of the mitral valve was not appreciated in control patients in the short axis valve plane with a representative example shown in Figure 6B.

LGE in the papillary muscles. Of the 19 prospectively enrolled MVP patients with adequate 3D LGE-CMR images, 16 were included in the analysis. Myocardial LGE was present in the papillary muscles in 10 of 16 MVP patients (63%) as indicated by 3D LGE-CMR, but 2D-LGE only identified 5 of those 10 (50%) patients (2 examples are shown in Fig. 7). There was no myocardial LGE found on 2D or 3D LGE-CMR in control patients. No additional myocardial LGE was observed in MVP

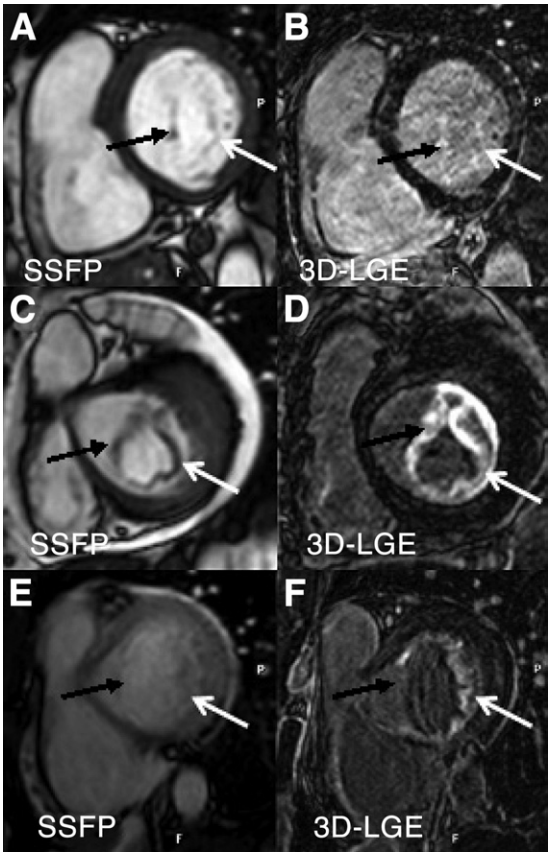

Figure 6. Mitral Valve LGE

(A, B) Control subject steady state free processing (SSFP) and late gadolinium enhancement (LGE) images at the short axis valve plane. In LGE, a very faint bright line represents normal valve leaflets. **Panel C** shows the SSFP image of a MVP patient with thickened leaflets. **Panel E** shows the SSFP image of another MVP patient who does not have readily identifiable leaflets. **Panels D and F** show the corresponding 3-dimensional LGE-CMR images with enhancement in the anterior leaflets **(black arrows)** and posterior leaflets **(white arrows)** in both patients. Abbreviations as in Figure 1.

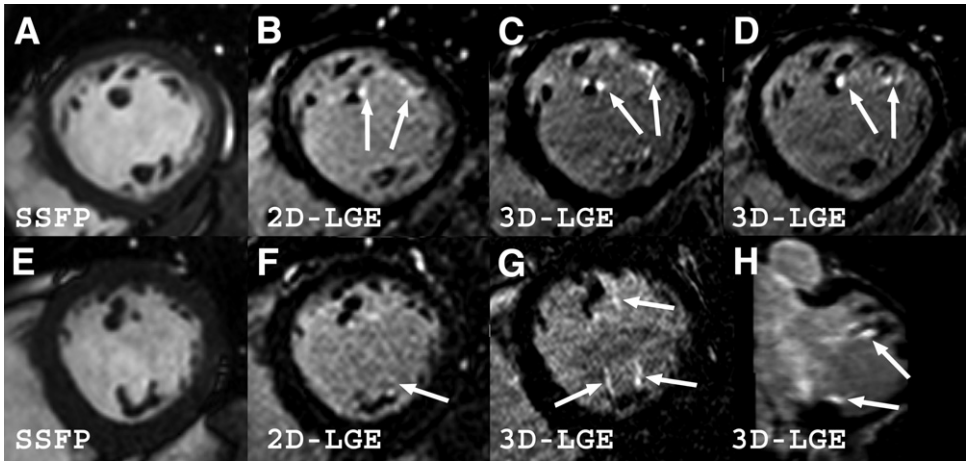

Figure 7. Mitral Papillary Muscle LGE

(A to D) Short axis SSFP, two-dimensional (2D) LGE-CMR, and high-resolution three-dimensional (3D) LGE-CMR images of 1 MVP patient at the mid-papillary muscle level. **Arrows** point to LGE. **(E to H)** Images from another MVP patient. **(E)** Short-axis SSFP. **(F)** A 2D LGE-CMR image with **(arrow)** "partial loss" of papillary muscle from volume averaging. **(G)** A 3D LGE-CMR. **(H)** A 3D multiplanar reconstruction confirming enhancement in the papillary muscle. **Arrows** point to LGE in the papillary muscle.

patients. We did not find significant difference in age, gender, EF, or MR grade in MVP patients with or without papillary muscle LGE (Table 4).

Arrhythmia history of these 16 patients showed 11 (69%) had either Holter monitor or loop monitor studies in the previous 5 years. All 8 patients with Grade IIIa (couplets) and IIIb (nonsustained ventricular tachycardia) CVA had positive LGE in papillary muscles. The remaining 3 patients with either no ventricular arrhythmia or a few isolated ventricular ectopic beats, but had no LGE on papillary muscles. There was a significant association between CVA and the presence of LGE in the papillary muscles ($p = 0.007$) (Table 5).

DISCUSSION

Cardiovascular magnetic resonance imaging is widely used to quantify LV function and MR volume (8–11,31,32) and recently has been used in imaging MVP (13), but CMR criterion for MVP is still lacking. In our present study, we applied TTE criteria for MVP to cine CMR images and found the criterion of 2 mm of mitral leaflet excursion into the left atrium beyond the mitral annulus in the long-axis view to be an applicable criterion in CMR. Using cine SSFP LVOT stack, we can identify prolapse within each scallop of the mitral valve and thus provide detailed valvular morphology information for surgical planning.

We found that MVP patients had thicker and longer posterior leaflets and larger MADs on CMR, with excellent correlation with TTE findings, which are consistent with published results (20,33,34). We did not find significant differences in the mitral anterior leaflet thickness or length in MVP and control patients by CMR imaging in our cohort. In pathological studies, the reported average control leaflet thickness was 1 mm and the average MVP leaflet thickness was 2 mm (35). The normal leaflet thickness is below the limit of spatial resolution achieved in routine CMR clinical imaging. Partial volume averaging has a greater affect on normal leaflets because of the thinner leaflets that make border identification for leaflet thickness measurements difficult. Unlike thickness measurements, the blood-to-leaflet contrast ratio does not depend on border identification and is readily mea-

Table 4. Patient Characteristics for LGE

	Control (n = 10)	MVP Patients (n = 16)		p Value
Age (yrs)	43.9 ± 11.7	51.4 ± 9.0		0.12*
Male (%)	5 (50)	9 (56)		0.77†
BSA (m^2)	1.86 ± 0.19	1.93 ± 0.26		0.49*
EF (%)	63.3 ± 5.0	64.6 ± 6.5		0.40*
MR (median)	1+	3+		<0.001†
		LGE+ (n = 10)	LGE− (n = 6)	
Age (yrs)		48.9 ± 9.8	55.2 ± 6.3	0.18*
Male (%)		6 (60)	3 (50)	0.71†
EF (%)		65.0 ± 7.1	64.0 ± 5.9	0.55*
MR (median)		3+	3+	0.91†

Values are mean ± standard deviation. *Student *t* test. †Wilcoxon rank sum test.
LGE = late gadolinium enhancement; other abbreviations as in Table 1.

Table 5. LGE and CVA in MVP Patients

LGE in Papillary Muscle	CVA (≥III)	Non-CVA (0, I)	Total
Yes	8	2	10
No	0	6	6
Total	8	8	16

Using Fisher's exact test, p = 0.007 for papillary muscle LGE and CVA. CVA = complex ventricular arrhythmia; other abbreviations as in Tables 1 and 4.

sured using standard CMR analysis software. In addition to an increased leaflet-to-blood contrast ratio, we also found that the MVP leaflets were frequently enhanced (94% of patients) in LGE-CMR images. Both of these findings may reflect the significantly expanded spongiosa layer with proteoglycan in the myxomatous valves (35).

We have found that LGE in the papillary muscles is associated with CVAs. Signal enhancement usually is present at the papillary muscle tips adjacent to the attachment of the chordae tendineae. The LGE has not been previously reported in MVP patients, which may be due to the challenge of identifying papillary fibrosis against a background of blood signals with significant partial volume averaging of blood and papillary muscles due to low spatial resolution in routine 2D LGE-CMR imaging. The 3D LGE-CMR image has the advantage of increased spatial resolution (nearly a 4-fold increase as 3D LGE-CMR voxel size is 0.26 of the 2D voxel size), particularly slice resolution (27,36), which is critical in the assessment of small regions of interest such as the papillary muscles. Furthermore, there was increased time delay between contrast injection and imaging for 3D LGE-CMR imaging compared with 2D LGE-CMR imaging, with possibly increased signal difference between blood and fibrosis (37).

Study limitations. We had no anterior-leaflet-only prolapse patients in our cohort, although the composition of our patient cohort is not unique (38). One possible explanation for this is that we excluded patients with aortic regurgitation, which seems to be associated with anterior leaflet prolapse (19). To further confirm that the 2-mm criterion should be used in the definition of MVP in CMR, a larger sample population and inclusion of patients with anterior-leaflet-only prolapse are necessary. The study of LGE and its association with CVAs is also limited by its small sample size. The risk of sudden death can only be assessed in a much larger patient cohort with long-term follow-up, which is beyond the scope of our study.

CONCLUSIONS

We have defined MVP in CMR by applying the TTE criterion—the excursion of any mitral leaflet segment(s) beyond the mitral annular plane into the left atrium during ventricular systole by at least 2 mm in the LVOT view. We have found that MVP patients, as compared with patients without MVP, have increased blood-to-leaflet contrast ratios, longer and thicker posterior leaflets, and enlarged MADs by CMR. We also report that hyperenhancement of the papillary muscles on LGE-CMR imaging is present in a subgroup of MVP patients with complex ventricular arrhythmias.

Reprint requests and correspondence: Dr. Yuchi Han, Cardiovascular Division, E/SH-457, Beth Israel Deaconess Medical Center, 330 Brookline Avenue, Boston, Massachusetts 02215. *E-mail: yhan@bidmc.harvard.edu.*

REFERENCES

1. Olson LJ, Subramanian R, Ackermann DM, Orszulak TA, Edwards WD. Surgical pathology of the mitral valve: a study of 712 cases spanning 21 years. Mayo Clin Proc 1987;62:22–34.
2. Levine RA, Triulzi MO, Harrigan P, Weyman AE. The relationship of mitral annular shape to the diagnosis of mitral valve prolapse. Circulation 1987;75:756–67.
3. Levine RA, Stathogiannis E, Newell JB, Harrigan P, Weyman AE. Reconsideration of echocardiographic standards for mitral valve prolapse: lack of association between leaflet displacement isolated to the apical four chamber view and independent echocardiographic evidence of abnormality. J Am Coll Cardiol 1988;11:1010–9.
4. Pepi M, Tamborini G, Maltagliati A, et al. Head-to-head comparison of two- and three-dimensional transthoracic and transesophageal echocardiography in the localization of mitral valve prolapse. J Am Coll Cardiol 2006;48:2524–30.
5. Muller S, Muller L, Laufer G, et al. Comparison of three-dimensional imaging to transesophageal echocardiography for preoperative evaluation in mitral valve prolapse. Am J Cardiol 2006;98:243–8.
6. Levine RA, Handschumacher MD, Sanfilippo AJ, et al. Three-dimensional echocardiographic reconstruction of the mitral valve, with implications for the diagnosis of mitral valve prolapse. Circulation 1989;80:589–98.
7. Flachskampf FA, Chandra S, Gaddipatti A, et al. Analysis of shape and motion of the mitral annulus in subjects with and without cardiomyopathy by echocardiographic 3-dimensional reconstruction. J Am Soc Echocardiogr 2000;13:277–87.
8. Chuang ML, Hibberd MG, Salton CJ, et al. Importance of imaging method over imaging modality in noninvasive determination of left ventricular volumes and ejection fraction: assessment by two- and three-dimensional echocardiography and magnetic resonance imaging. J Am Coll Cardiol 2000;35:477–84.

9. Salton CJ, Chuang ML, O'Donnell CJ, et al. Gender differences and normal left ventricular anatomy in an adult population free of hypertension. A cardiovascular magnetic resonance study of the Framingham Heart Study Offspring cohort. J Am Coll Cardiol 2002;39:1055–60.
10. Fujita N, Chazouilleres AF, Hartiala JJ, et al. Quantification of mitral regurgitation by velocity-encoded cine nuclear magnetic resonance imaging. J Am Coll Cardiol 1994;23:951–8.
11. Kon MW, Myerson SG, Moat NE, Pennell DJ. Quantification of regurgitant fraction in mitral regurgitation by cardiovascular magnetic resonance: comparison of techniques. J Heart Valve Dis 2004;13:600–7.
12. Gelfand EV, Hughes S, Hauser TH, et al. Severity of mitral and aortic regurgitation as assessed by cardiovascular magnetic resonance: optimizing correlation with Doppler echocardiography. J Cardiovasc Magn Reson 2006;8:503–7.
13. Stork A, Franzen O, Ruschewski H, et al. Assessment of functional anatomy of the mitral valve in patients with mitral regurgitation with cine magnetic resonance imaging: comparison with transesophageal echocardiography and surgical results. Eur Radiol 2007;17:3189–98.
14. Marks AR, Choong CY, Sanfilippo AJ, Ferre M, Weyman AE. Identification of high-risk and low-risk subgroups of patients with mitral-valve prolapse. N Engl J Med 1989;320:1031–6.
15. Nishimura RA, McGoon MD, Shub C, Miller FA Jr., Ilstrup DM, Tajik AJ. Echocardiographically documented mitral-valve prolapse. Long-term follow-up of 237 patients. N Engl J Med 1985;313:1305–9.
16. Hayek E, Gring CN, Griffin BP. Mitral valve prolapse. Lancet 2005;365:507–18.
17. Carpentier AF, Lessana A, Relland JY, et al. The "physio-ring": an advanced concept in mitral valve annuloplasty. Ann Thorac Surg 1995;60:1177–85; discussion 1185–6.
18. Suri RM, Schaff HV, Dearani JA, et al. Survival advantage and improved durability of mitral repair for leaflet prolapse subsets in the current era. Ann Thorac Surg 2006;82:819–26.
19. David TE, Ivanov J, Armstrong S, Christie D, Rakowski H. A comparison of outcomes of mitral valve repair for degenerative disease with posterior, anterior, and bileaflet prolapse. J Thorac Cardiovasc Surg 2005;130:1242–9.
20. Omran AS, Woo A, David TE, Feindel CM, Rakowski H, Siu SC. Intraoperative transesophageal echocardiography accurately predicts mitral valve anatomy and suitability for repair. J Am Soc Echocardiogr 2002;15:950–7.
21. Zuppiroli A, Mori F, Favilli S, et al. Arrhythmias in mitral valve prolapse: relation to anterior mitral leaflet thickening, clinical variables, and color Doppler echocardiographic parameters. Am Heart J 1994;128:919–27.
22. Vohra J, Sathe S, Warren R, Tatoulis J, Hunt D. Malignant ventricular arrhythmias in patients with mitral valve prolapse and mild mitral regurgitation. Pacing Clin Electrophysiol 1993;16:387–93.
23. Dollar AL, Roberts WC. Morphologic comparison of patients with mitral valve prolapse who died suddenly with patients who died from severe valvular dysfunction or other conditions. J Am Coll Cardiol 1991;17:921–31.
24. Corrado D, Basso C, Nava A, Rossi L, Thiene G. Sudden death in young people with apparently isolated mitral valve prolapse. G Ital Cardiol 1997;27:1097–105.
25. Farb A, Tang AL, Atkinson JB, McCarthy WF, Virmani R. Comparison of cardiac findings in patients with mitral valve prolapse who die suddenly to those who have congestive heart failure from mitral regurgitation and to those with fatal noncardiac conditions. Am J Cardiol 1992;70:234–9.
26. Chesler E, King RA, Edwards JE. The myxomatous mitral valve and sudden death. Circulation 1983;67:632–9.
27. Peters DC, Wylie JV, Hauser TH, et al. Detection of pulmonary vein and left atrial scar after catheter ablation with three-dimensional navigator-gated delayed enhancement MR imaging: initial experience. Radiology 2007;243:690–5.
28. Kim RJ, Fieno DS, Parrish TB, et al. Relationship of MRI delayed contrast enhancement to irreversible injury, infarct age, and contractile function. Circulation 1999;100:1992–2002.
29. Look D, Locker D. Time savings in measure of NMR and EPR relaxation times. Rev Sci Instrum 1970;41:250–1.
30. Lown B, Wolf M. Approaches to sudden death from coronary heart disease. Circulation 1971;44:130–42.
31. Alfakih K, Plein S, Thiele H, Jones T, Ridgway JP, Sivananthan MU. Normal human left and right ventricular dimensions for MRI as assessed by turbo gradient echo and steady-state free precession imaging sequences. J Magn Reson Imaging 2003;17:323–9.
32. Chatzimavroudis GP, Oshinski JN, Pettigrew RI, Walker PG, Franch RH, Yoganathan AP. Quantification of mitral regurgitation with MR phase-velocity mapping using a control volume method. J Magn Reson Imaging 1998;8:577–82.
33. Salustri A, Becker AE, van Herwerden L, Vletter WB, Ten Cate FJ, Roelandt JR. Three-dimensional echocardiography of normal and pathologic mitral valve: a comparison with two-dimensional transesophageal echocardiography. J Am Coll Cardiol 1996;27:1502–10.
34. Fyrenius A, Engvall J, Janerot-Sjoberg B. Major and minor axes of the normal mitral annulus. J Heart Valve Dis 2001;10:146–52.
35. Rabkin E, Aikawa M, Stone JR, Fukumoto Y, Libby P, Schoen FJ. Activated interstitial myofibroblasts express catabolic enzymes and mediate matrix remodeling in myxomatous heart valves. Circulation 2001;104:2525–32.
36. Saranathan M, Rochitte CE, Foo TK. Fast, three-dimensional free-breathing MR imaging of myocardial infarction: a feasibility study. Magn Reson Med 2004;51:1055–60.
37. Klein C, Nekolla SG, Balbach T, et al. The influence of myocardial blood flow and volume of distribution on late Gd-DTPA kinetics in ischemic heart failure. J Magn Reson Imaging 2004;20:588–93.
38. Mills WR, Barber JE, Skiles JA, et al. Clinical, echocardiographic, and biomechanical differences in mitral valve prolapse affecting one or both leaflets. Am J Cardiol 2002;89:1394–9.

APPENDIX

For the supplementary video, please see the online version of this article.